646 (1996); T. Pape, W. Wintermeyer, M. Rodnina, *EMBO J.* **18**, 3800 (1999).
3. T. Pape, W. Wintermeyer, M. V. Rodnina, *EMBO J.* **17**, 7490 (1998).
4. J. Davies, W. Gilbert, L. Gorini, *Proc. Natl. Acad. Sci. U.S.A.* **51**, 883 (1964).
5. R. Green and H. F. Noller, *Annu. Rev. Biochem.* **66**, 679 (1997).
6. D. Moazed and H. F. Noller, *Cell* **47**, 985 (1986); *J. Mol. Biol.* **211**, 135 (1990).
7. D. Moazed and H. F. Noller, *Nature* **327**, 389 (1987); R. Karimi and M. Ehrenberg, *Eur. J. Biochem.* **226**, 355 (1994).
8. D. Fourmy, M. I. Recht, S. C. Blanchard, J. D. Puglisi, *Science* **274**, 1367 (1996); D. Fourmy, S. Yoshizawa, J. D. Puglisi, *J. Mol. Biol.* **277**, 333 (1998); S. Yoshizawa, D. Fourmy, J. D. Puglisi, *EMBO J.* **17**, 6437 (1998); S. C. Blanchard, D. Fourmy, R. G. Eason, J. D. Puglisi, *Biochemistry* **37**, 7716 (1998).
9. U. von Ahsen and H. F. Noller, *Science* **267**, 234 (1995).
10. Biotin was attached to the 3′ end of yeast $tRNA^{Phe}$ (Sigma) as previously described (*9*). The gene32 mRNA fragment corresponding to positions −55 to +85 and *E. coli* ribosomal subunits was prepared with standard methods. Binding of biotin-$tRNA^{Phe}$ to the A site was confirmed by chemical probing of 30*S* subunits (*6*). A-site or P-site biotin-$tRNA^{Phe}$-ribosome complexes were captured by incubation for 20 min at room temperature with magnetic streptavidin beads (streptavidin-M280; Dynal; 12.5 μg of beads per 1 pmol of biotin-$tRNA^{Phe}$). The beads were prewashed three times with buffer containing 0.3% bovine serum albumin (BSA) and once with buffer lacking BSA, and the unbound subunits were removed by washing three times with the 20 μl of binding buffer after the beads were trapped with a magnet.
11. S. Watanabe, *J. Mol. Biol.* **67**, 443 (1972); R. Lill, J. M. Robertson, W. Wintermeyer, *Biochemistry* **25**, 3245 (1986).
12. D. Hartz, D. S. McPheeters, R. Traut, L. Gold, *Methods Enzymol.* **164**, 419 (1988). For toeprinting, gene 32 mRNA was annealed to 5′ ^{32}P–end-labeled primer as described. The A-site complex was formed with 5 pmol of mRNA, 10 pmol of 30*S* subunit, 50 pmol of $tRNA^{fMet}$, and 10 pmol of biotin-$tRNA^{Phe}$ in 12 μl of selection buffer [80 mM potassium cacodylate (pH 7.2), 150 mM NH_4Cl, 1 mM dithiothreitol, and 12 mM $MgCl_2$]. The P-site complex was formed by excluding $tRNA^{fMet}$. The A-site or P-site complex was captured with magnetic streptavidin beads as in (*10*). Primer extension was performed directly on the beads.
13. For modification-interference experiments, 30*S* subunits (320 pmol) were first modified with dimethyl sulfate (DMS), kethoxal, or 1-cyclohexyl-3-(2-morpholinoethyl)carbodiimide metho-*p*-toluenesulfonate at 37°C for 10 min (*6*). Reagents were subsequently removed by spinning with microcon 30 (Amicon). The A-site or P-site complex was formed with 100 pmol of 30*S* subunits, 250 pmol of mRNA, with or without 500 pmol of $tRNA^{fMet}$, and 50 pmol of biotin-$tRNA^{Phe}$ in 20 μl of selection buffer. For selection in the presence of paromomycin, 100 μM drug was added. The active subunits were captured with beads and released by addition of 20 μl of 5 mM EDTA, 0.5% SDS, and 300 mM sodium acetate (pH 5.4) and incubation at room temperature for 20 min. Modifications were detected by primer extension with 12 independent primers to scan the entire sequence of 16*S* rRNA. Modification levels were quantified with a Phosphorimager (Molecular Dynamics), normalized to account for differences in lane loadings, and background levels estimated from unmodified sample lanes were subtracted. Modification of the same set of nucleotides as observed in (*9*) interfered with P-site tRNA binding, except that the interference at G1401 (N7) was not observed.
14. T. Powers and H. F. Noller, *Trends Genet.* **10**, 27 (1994).
15. Oligonucleotide-directed mutations were constructed in pBS-V as described (*16*). Mutations were introduced into an expression plasmid that contains the rrnB operon under control of phage lambda P_L promoter and cI857, a thermolabile allele of the lambda repressor. Strain DH1 was used as the recipient of the final constructs.
16. M. I. Recht, S. Douthwaite, K. D. Dahlquist, J. D. Puglisi, *J. Mol. Biol.* **286**, 33 (1999).
17. The A-site complex was formed by incubating the mixture of mutant 30*S* subunits and wild-type subunits (50 pmol total), 250 pmol of gene32 mRNA, 250 pmol of $tRNA^{fMet}$, and 10 pmol of $tRNA^{Phe}$ in 10 μl of selection buffer. The ratio between mutant and wild-type ribosomal subunit population was analyzed by primer extension from allele-specific priming site V as described (*16*). The mutant population in each mixture was A1492G, 40 ± 3%; A1492C, 40 ± 2%; A1493G, 32 ± 2%; A1493C, 23 ± 3%; A1492G-A1493G, 32 ± 3%; and A1492C-A1493C, 43 ± 2%.
18. S. Yoshizawa and J. D. Puglisi, unpublished results.
19. R. A. Grajevskaja, Y. V. Ivanov, E. M. Saminsky, *Eur. J. Biochem.* **128**, 47 (1982); S. V. Kirillow, E. M. Makarov, Y. Semenkov, *FEBS Lett.* **157**, 91 (1983); R. Lill, J. M. Robertson, W. Wintermeyer, *Biochemistry* **23**, 6710 (1984).
20. B. J. McCarthy and J. J. Holland, *Proc. Natl. Acad. Sci. U.S.A.* **54**, 880 (1965); H. Aurup, A. Siebert, F. Benseler, D. Williams, F. Eckstein, *Nucleic Acids Res.* **22**, 4963 (1994).
21. A. P. Patapov, F. J. Triana-Alonso, K. Nierhaus, *J. Biol. Chem.* **270**, 17680 (1995).
22. A. M. Pyle, F. L. Murphy, T. R. Cech, *Nature* **358**, 123 (1992).
23. K. Brady, A. Wei, D. Ringe, R. H. Abeles, *Biochemistry* **29**, 7600 (1990); T. R. Burke *et al.*, *ibid.* **35**, 15989 (1996); L. H. Takahashi, R. Radhakrishnan, R. E. Rosenfield Jr., E. F. Meyer Jr., D. A. Trainor, *J. Am Chem. Soc.* **111**, 3368 (1989).
24. The 2′ fluoro- and 2′ deoxy-U mRNAs were transcribed with $Tyr^{639} \rightarrow$ Phe mutant T7 RNA polymerase (*29*) with 2′ fluoro uridine triphosphate (UTP) (Amersham) or 2′ deoxy-UTP (Sigma) as substrates.
25. S. Doublié, S. Tabor, A. M. Long, C. C. Richardson, T. Ellenberger, *Nature* **391**, 251 (1998).
26. M. S. VanLoock, T. R. Easterwood, S. C. Harvey, *J. Mol. Biol.* **285**, 2069 (1999).
27. A. A. Szewczak, L. Ortoleva-Donnelly, S. P. Ryder, E. Moncoeur, S. A. Strobel, *Nature Struct. Biol.* **5**, 1037 (1998); G. J. Narlikar and D. Herschlag, *Biochemistry* **37**, 9902 (1998).
28. J. S. Lodmell and A. E. Dahlberg, *Science* **277**, 1262 (1997).
29. R. Sousa and R. Padilla, *EMBO J.* **14**, 4609 (1995).
30. The authors thank H. Noller, S. Joseph, R. Green, M. Recht, K. Dahlquist, and S. Blanchard for assistance and helpful discussions and R. Sousa for the plasmid encoding the $Tyr^{639} \rightarrow$ Phe mutant T7 RNA polymerase gene. Supported by grants from NIH (GM51266), the Packard Foundation, and the Lucille P. Markey Charitable Trust. S.Y. was supported by a grant from the Japan Society for the Promotion of Science. D.F. was supported by a grant from Institut National de la Santé et de la Recherche Médicale.

1 June 1999; accepted 9 August 1999

Activity-Induced Potentiation of Developing Neuromuscular Synapses

Ji-jun Wan and Mu-ming Poo*

Electrical activity plays a critical role in shaping the structure and function of synaptic connections in the nervous system. In *Xenopus* nerve-muscle cultures, a brief burst of action potentials in the presynaptic neuron induced a persistent potentiation of neuromuscular synapses that exhibit immature synaptic functions. Induction of potentiation required an elevation of postsynaptic Ca^{2+} and expression of potentiation appeared to involve an increased probability of transmitter secretion from the presynaptic nerve terminal. Thus, activity-dependent persistent synaptic enhancement may reflect properties characteristic of immature synaptic connections, and bursting activity in developing spinal neurons may promote functional maturation of the neuromuscular synapse.

Electrical activity can induce modifications of synaptic connections in developing and mature nervous systems (*1*). In various parts of the central nervous system, a brief period of repetitive synaptic activity induces a persistent increase or decrease in synaptic efficacy (*2*), known as long-term potentiation (LTP) or long-term depression (LTD). At developing neuromuscular synapses in culture, a form of persistent heterosynaptic depression similar to LTD can be induced by repetitive stimulation of an adjacent neuron coinnervating the same muscle cell (*3*). Persistent depression can also be induced by repetitive activation of postsynaptic acetylcholine (ACh) receptors with iontophoresis of ACh (*4*) or by a brief elevation of postsynaptic Ca^{2+} through release of caged Ca^{2+} (*5*). However, a phenomenon similar to LTP has not been reported in any neuromuscular system. In this work, we have identified conditions under which repetitive activity can induce persistent enhancement of synaptic transmission at developing neuromuscular synapses in a cell culture preparation.

We made simultaneous whole-cell perforated patch recordings from presynaptic spinal neurons and postsynaptic myocytes in 1-day-old *Xenopus* nerve-muscle cultures (*6*). We assayed the synaptic efficacy by measuring the mean amplitude of excitatory postsynaptic currents (EPSCs) evoked by test stimuli at a low frequency (0.05 Hz) (*7*). For

Department of Biology, University of California at San Diego, La Jolla, CA 92093, USA.

*To whom correspondence should be addressed. E-mail: mpoo@ucsd.edu

induction of synaptic changes, we initiated a burst of five action potentials (at a frequency of 10 or 40 Hz) in the presynaptic neuron by injecting depolarizing current pulses (termed burst stimulation), while the postsynaptic myocyte was held in either current or voltage clamp (*8*). We consistently observed an increase in the amplitude of EPSCs after the burst stimulation for synapses that exhibited EPSCs with initial mean amplitudes less than 1.5 nA (Fig. 1, A and B). The appearance of potentiation had a slow onset, reaching a plateau value about 20 to 30 min after the burst, and persisted for as long as a stable recording could be made (up to 80 min after the burst). In most cases, no change in the EPSC amplitude was observed during the period immediately after the burst. In the absence of burst stimulation, the mean EPSC amplitude showed no significant change during the 1-hour period of the experiment (Fig. 1B). The degree of potentiation was inversely correlated with the initial synaptic strength (Fig. 1C) and positively correlated with the coefficient of variation (CV) of the initial EPSC amplitude (*9*), which measures the extent of fluctuation and decreases with increasing strength and reliability of the synapse. Synaptic transmission at immature neuromuscular synapses is characterized by EPSCs of low amplitude and high fluctuation, with frequent transmission failure (*10*). Thus, immature synapses appear to be more susceptible to potentiation by a burst of synaptic activity.

In the absence of presynaptic action potentials, quantal packets of ACh are released spontaneously, as indicated by miniature EPSCs (mEPSCs) recorded in the myocyte (*11*). The frequency and amplitude distribution of mEPSCs before and after burst stimulation showed a clear increase in the frequency of mEPSCs (Fig. 2A), whereas the mean amplitude, amplitude distribution, and time course of mEPSCs did not show any significant change (Fig. 2B). This suggests that burst stimulation resulted in enhanced probability of quantal transmitter secretion without any change in postsynaptic sensitivity to the transmitter. That enhanced presynaptic release may account for the increase in the EPSC amplitude is further supported by the observation that the gradual increase in the mEPSC frequency correlates with that in the EPSC amplitude (Figs. 1B and 2A). However, it is possible that the gradual enhancement of EPSCs after burst stimulation was due to the appearance of new postsynaptic ACh

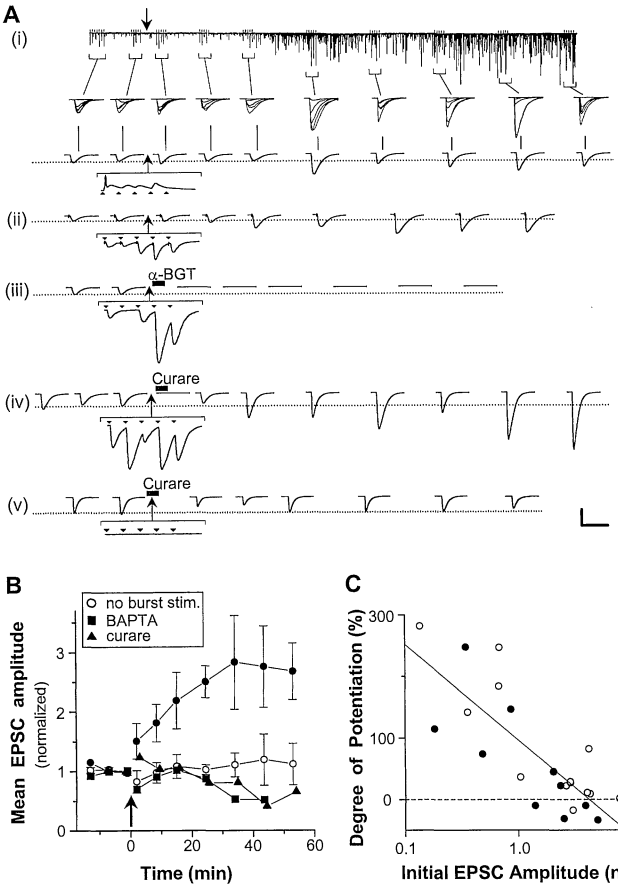

Fig. 1. Persistent synaptic potentiation induced by burst stimulation. (**A**) Continuous trace in (i) represents membrane current recorded from an innervated myocyte ($V_c = -70$ mV). A train of test stimuli (0.05 Hz; five to seven pulses) was applied every 6 to 9 min at the times marked by short vertical bars and the EPSCs elicited were shown at higher resolution as the superimposed traces. The average of these five to seven events is also shown below (dotted line, average amplitude of EPSCs during the control period). In (ii) to (v), only averaged traces of EPSCs at various times before and after burst stimulation are shown. The burst was initiated in the presynaptic neuron (40 Hz; five pulses) at the time marked by the arrow, when the myocyte was under current clamp (i) or voltage clamp (ii to v). Traces of membrane depolarization (i) or EPSCs (ii to v) during the burst stimulation are shown below. Action potentials within the burst were triggered in the presynaptic neuron at the times marked by small arrowheads. In (iii) to (v), a pulse of α-BGT (50 μg/ml; RBI) or *d*-tubocurarine (curare) (15 mM; Sigma) was pressure-ejected near the synapse (horizontal bar) after (iii and iv) or during (v) burst stimulation. Scales: 1 nA, 4 min for the slow trace; 1 nA, 40 ms for fast EPSCs; 100 mV, 40 ms for depolarizations. (**B**) Summary of all experiments similar to that in (A). Mean EPSC amplitudes at various times before and after burst stimulation were normalized to the mean value observed before the burst at the same synapse and grouped into 6- to 9-min bins. Data represent mean ± SEM. Filled circles ($n = 9$), burst stimulation (five pulses, 10 to 40 Hz) was applied at time 0 (arrow); open circles ($n = 8$), control experiments with no burst stimulation; filled squares ($n = 10$), myocytes were loaded with BAPTA (5 mM); filled triangles ($n = 4$), curare was applied during burst stimulation (five pulses; 40 Hz). In all experiments, the initial mean EPSC amplitudes were <1.5 nA. (**C**) Degree of potentiation, defined by percentage change in the mean EPSC amplitude 15 to 45 min after burst stimulation, plotted against the initial mean amplitude of EPSCs. Line represents the best linear fit of the data ($r = -0.80$; $P < 0.0001$). Open and filled circles are data obtained for burst stimulation at 10 and 40 Hz (five pulses), respectively.

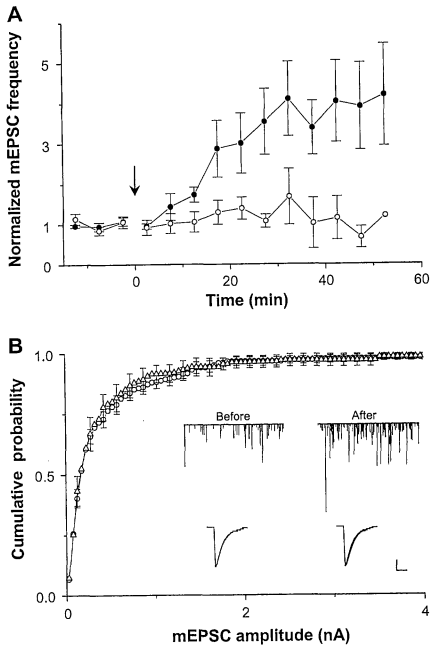

Fig. 2. (**A**) Summary of changes in the mEPSC frequency induced by burst stimulation. Frequency values were normalized against the mean frequency before the burst. Filled circles ($n = 7$), synapses treated with the burst stimulation at the time marked by the arrow; open circles ($n = 6$), controls (no burst stimulation). (**B**) Distribution of mEPSC amplitudes before and after induction of persistent potentiation. Cumulative probability during a 5-min period before (circles) and during a 15- to 20-min period after (triangles) the burst. Values represent mean ± SEM from seven experiments. The difference between the two sets of data was not significant ($P > 0.1$; Kolmogorov-Smirnov test). (Insets) Sample 5-min traces of the myocyte membrane current before and after the burst. Trace below represents the average of all mEPSCs recorded during the 5-min period, with two traces superimposed on the right. Data of the mEPSC frequency and amplitude were obtained from experiments described in Fig. 1. Scale: slow traces, 0.2 nA, 30 s; fast traces, 50 pA, 10 ms.

receptor clusters in a manner that was not reflected by any change in the mEPSC amplitude, reminiscent of the silent synapse hypothesis (*12*). Because there was a gradual development of potentiation after the burst (Figs. 1 and 2A), we further examined whether new receptors had appeared gradually after the burst. A brief pulse of α-bungarotoxin (α-BGT), an irreversible blocker of ACh receptors, was applied to the culture immediately after burst stimulation (Fig. 1Aiii). No appearance of new ACh receptors was observed after α-BGT was cleared from the culture ($n = 4$). Application of the drug and extensive washing of the culture did not result in any adverse effects, as shown by the normal appearance of potentiation when *d*-tubocurarine, a reversible blocker of ACh receptors, was used instead of α-BGT (Fig. 1Aiv). Although the potentiation is expressed as an increased transmitter secretion, the induction of potentiation appears to require postsynaptic activation of ACh receptors because we observed no potentiation when curare was present during burst stimulation ($n = 4$) (Fig. 1, Av and B). Activation of ACh receptors after burst stimulation is not essential for induction of potentiation because curare application after the burst for a prolonged period (30 min) did not interfere with the appearance of potentiation, which was immediately revealed after curare was removed (*13*).

When we varied the frequency of action potentials induced within the burst while keeping the total number of action potentials constant, we observed significant potentiation when the frequency was 0.6 Hz or higher (Fig. 3A). We then varied the total number of stimuli within the burst and kept the frequency of action potentials constant at 10 Hz. We observed significant potentiation when the total number of stimuli was 5 or more and the extent of potentiation was not significantly different for 5, 15, and 50 stimuli (Fig. 3B).

Repetitive activation of the neuromuscular synapse causes an influx of Ca^{2+} through activated ACh channels, and such Ca^{2+} influx is necessary for induction of the persistent synaptic depression (*3, 4*). We thus examined whether Ca^{2+} influx into the postsynaptic myocyte is also necessary for induction of persistent potentiation by burst stimulation. When a Ca^{2+}

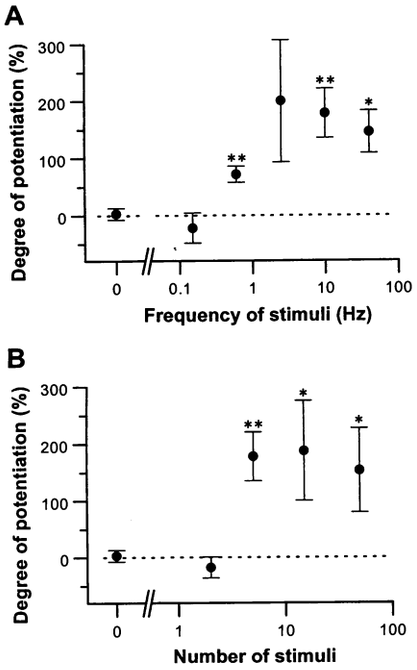

Fig. 3. Dependence of synaptic potentiation on the pattern of burst stimulation. Degree of potentiation was defined by the percentage change in the mean amplitude of EPSCs 15 to 45 min after the burst. Each point represents the average value obtained from four to eight experiments. (**A**) The number of action potentials initiated was kept constant at five and the frequency within the burst was varied from 0.15 to 40 Hz. (**B**) The frequency of action potentials in the burst was kept constant at 10 Hz and the number of action potentials was varied from 2 to 50. All data points represent mean ± SEM. Asterisks mark data that are significantly different from the control (plotted at 0 Hz or 0 pulse number) (*, $P < 0.05$; **, $P < 0.01$; *t* test). All synapses exhibited EPSCs with initial mean amplitudes less than 1.5 nA.

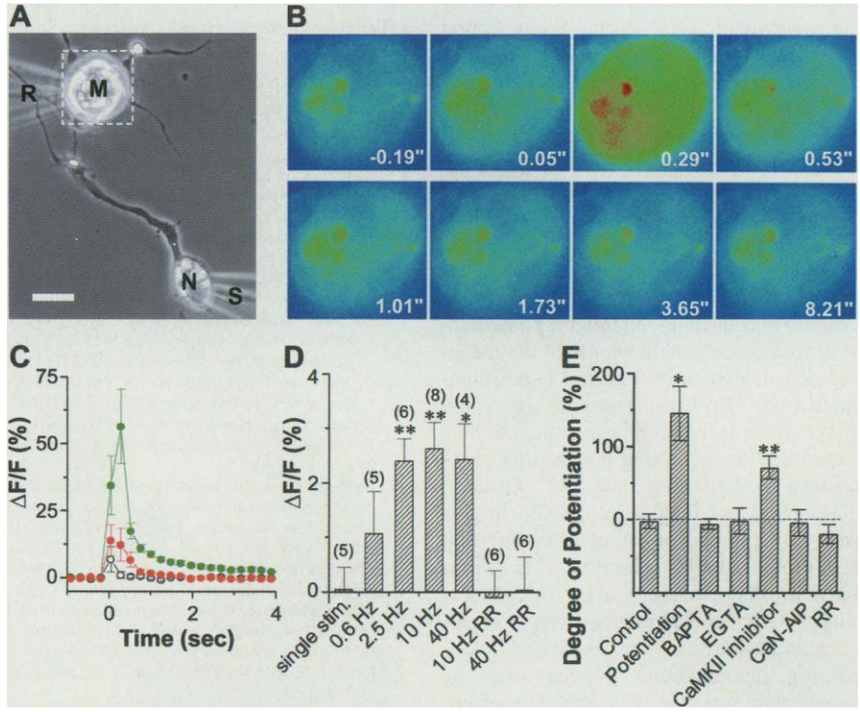

Fig. 4. Postsynaptic Ca^{2+} elevation induced by burst stimulation. (**A**) A phase-contrast image of an innervated *Xenopus* myocyte (M), presynaptic neuron (N), whole-cell recording pipette (R), and stimulating pipette (S). Scale bar, 20 μm. (**B**) Change of Ca^{2+} concentration in the myocyte, as indicated by fluo-3 fluorescence, was sampled over the entire myocyte [dashed box in (A)] at different times (marked by the number in seconds) after burst stimulation at $t = 0$ (10 Hz; five pulses). The myocyte was loaded with fluo-3 and voltage clamped at −70 mV (*14*). (**C**) Percentage change ($\Delta F/F$) in the intensity of fluo-3 fluorescence from the entire myocyte was measured before and after burst stimulation at 10 Hz (five pulses) without (green circles, $n = 8$) or with (red circles, $n = 6$) intracellular loading of ruthenium red in the myocyte. Fluorescence changes induced by a single presynaptic stimulus are also shown (open circles; $n = 5$). Data points represent mean ± SEM. (**D**) Persistent elevation of postsynaptic Ca^{2+} induced by burst stimuli at different frequencies (0.6 to 40 Hz; all five pulses). Changes in the fluo-3 fluorescence were averaged between 2 and 10 s after the last stimulus in the burst. For two frequencies (10 and 40 Hz), the effects of intracellular loading of ruthenium red (RR) in the postsynaptic myocyte are also shown. Bars represent mean ± SEM. Number of experiments is shown in parentheses. Asterisks mark data that are significantly different from that of the single stimulation (*, $P < 0.05$; **, $P < 0.01$; *t* test). (**E**) Effects of postsynaptic manipulation on induction of synaptic potentiation. Burst stimulation (40 Hz; five pulses) was applied in all experiments except the controls. BAPTA (5 mM) (buffered with 2 mM $CaCl_2$), EGTA (5 mM) (buffered with 2 mM $CaCl_2$), [Ala^{286}]Ca^{2+}calmodulin kinase II inhibitor(281–301) (200 μM), calcineurin inhibitor (CaN-AIP, 250 μM), or ruthenium red (RR, 50 μM) was loaded into the postsynaptic myocyte for at least 15 min before the burst was applied. Asterisks indicate data that are significantly different from control (no burst stimulation; *, $P < 0.05$; **, $P < 0.01$; *t* test). All synapses in (E) exhibited EPSCs with initial mean amplitudes less than 1.5 nA.

chelator, 1,2-bis(2-aminophenoxy)ethane-*N*,*N*,*N*′,*N*′-tetraacetic acid (BAPTA), was loaded into the postsynaptic myocyte, the standard burst stimulation (40 Hz, five pulses) was no longer effective in inducing any synaptic change (Fig. 1B). We also directly monitored changes in the amount of Ca^{2+} in the myocyte by using fluo-3 loaded through a whole-cell patch electrode (*14*). Burst stimulation (10 Hz, five pulses) of the presynaptic neuron induced a transient increase in the fluo-3 fluorescence (Fig. 4), indicating increased Ca^{2+} in the myocyte. The fluo-3 fluorescence decayed to a steady level above the baseline and persisted for at least 10 s after the burst. When various patterns of the burst were tested, a small but persistent elevation of the postsynaptic Ca^{2+} during the postburst period was found for those patterns capable of inducing synaptic potentiation (Figs. 3A and 4D). This persistent Ca^{2+} elevation produced by the burst appeared to result from Ca^{2+}-induced Ca^{2+} release, because it was abolished by intracellular loading of ruthenium red (Fig. 4, C and D), an inhibitor of this release process (*15*).

Is Ca^{2+} release from internal stores responsible for induction of potentiation? Loading of ruthenium red into the postsynaptic myocyte completely abolished the induction of potentiation by standard burst stimulation (Fig. 4E). Consistent with the notion that a slow increase in cytosolic Ca^{2+} is responsible for triggering potentiation, postsynaptic loading of a slow Ca^{2+} chelator, EGTA, was as effective as BAPTA in preventing the induction of potentiation (Fig. 4E). Prolonged Ca^{2+} elevation is known to activate calcineurin (*16*), a Ca^{2+}-dependent phosphatase involved in hippocampal synaptic plasticity (*17*). When we loaded a calcineurin autoinhibitory peptide into the postsynaptic myocyte (*18*), induction of potentiation was completely blocked (Fig. 4E). In contrast, similar loading of a peptide inhibitor of another Ca^{2+}-dependent enzyme, Ca^{2+}-calmodulin–dependent protein kinase II (CaMKII), did not significantly affect the induction of potentiation (Fig. 4E). Interestingly, loading of the same inhibitory peptide of CaMKII blocked induction of the persistent depression at these synapses (*19*). In the CA1 area of the hippocampus, CaMKII is required for induction of LTP, whereas calcineurin is required for induction of LTD (*17*, *20*), a situation opposite that found here.

Bursting activity with frequency of action potentials in the range of 10 to 60 Hz has been observed in the developing spinal cord (*21*). Our results suggest that such activity in spinal motor neurons may be effective in potentiating developing neuromuscular junctions. Through immediate modification of the existing transmitter secretion machinery, the bursting activity could promote functional maturation of the synapse. Our finding that persistent potentiation can be induced only at immature neuromuscular junctions suggests that this form of synaptic plasticity is intimately tied to the immaturity of the synapse, presumably in the transmitter release mechanism of the presynaptic nerve terminal. Presynaptic modification of transmitter release accounts for the potentiation induced by burst stimulation as well as the persistent depression induced by repetitive heterosynaptic activity (*3*). In both cases, however, the induction of synaptic modification requires postsynaptic elevation of Ca^{2+} concentration. Thus, retrograde signaling is essential for both up- and down-regulation of synaptic efficacy of these developing synapses. The pattern of synaptic activity, as reflected by changes in postsynaptic Ca^{2+}, represents a critical determinant for the nature of retrograde signals.

References and Notes

1. C. S. Goodman and C. J. Shatz, *Cell* **72**/*Neuron* **10** (suppl.), 77 (1993).
2. T. V. P. Bliss and T. Lømo, *J. Physiol. London* **232**, 331 (1973); T. V. P. Bliss and G. L. Collingridge, *Nature* **361**, 31 (1993); D. J. Linden and J. A. Connor, *Annu. Rev. Neurosci.* **18**, 319 (1995); R. A. Nicoll and R. C. Malenka, *Nature* **377**, 115 (1995). L. Zhang, H-z. Tao, C. Holt, W. Harris, M-m. Poo, *ibid.* **395**, 37 (1998).
3. Y.-J. Lo and M.-m. Poo, *Science* **254**, 1019 (1991); Y. J. Lo and M.-m. Poo, *J. Neurosci.* **14**, 4684 (1994).
4. Y. Dan and M.-m. Poo, *Science* **256**, 1570 (1992).
5. S. Cash, Y. Dan, M.-m. Poo, R. S. Zucker, *Neuron* **16**, 745 (1996); S. Cash, R. S. Zucker, M.-m. Poo, *Science* **272**, 998 (1996).
6. *Xenopus* nerve-muscle cultures were prepared as described [N. Tabti, J. Alder, M.-m. Poo, in *Culturing Nerve Cells*, G. Banker and K. Goslin, Eds. (MIT Press, Cambridge, MA, ed. 2, 1998), pp. 237–260]. The cells were plated on clean glass cover slips and cultured for 1 day at room temperature (20° to 22°C) before use. The culture medium consisted of (v/v) 50% Leibovitz's medium (L-15; Gibco), 1% fetal bovine serum (Gibco), and 49% Ringer's solution [115 mM NaCl, 2 mM $CaCl_2$, 2.5 mM KCl, 10 mM Hepes (pH 7.3)].
7. Low-frequency test stimulation was used to minimize test-induced synaptic depression at these developing synapses [see (*3*)].
8. Synaptic currents were recorded from innervated muscle cells by whole-cell recording methods with an Axopatch 1D amplifier. The recordings were made at room temperature in a bath solution containing 140 mM NaCl, 5 mM KCl, 1 mM $CaCl_2$, 1 mM $MgCl_2$, and 10 mM Hepes (pH 7.4). The intrapipette solution contained 145 mM KCl, 1 mM NaCl, 1 mM $MgCl_2$, 1 mM adenosine triphosphate, and 10 mM Hepes (pH 7.2). For perforated-patch whole-cell recording, the pipette solution for the myocyte contained 125 mM potassium gluconate, 20 mM KCl, 1 mM NaCl, 1 mM $MgCl_2$, 10 mM Hepes, and amphotericin B at 200 μg/ml (pH 7.2); the solution for the neuron had similar composition except that it included 140 mM potassium gluconate and no KCl was used. The presynaptic neuron was under current clamp during the experiment. We triggered action potentials in the neuron by injecting current pulses (1 to 2 ms; 1 to 1.5 nA). For perforated-patch myocyte recording under voltage clamp, series resistance (5 to 8 MΩ) was always compensated at 80% to 85% (lag, 10 μs). In a typical experiment, 10 to 15 min of stable control recording was obtained before burst stimulation was applied. The membrane current recorded was filtered at 1 kHz, digitized by an interface, and acquired with a microcomputer for further analysis using SCAN and WCP programs (kindly provided by J. Dempster, University of Strathclyde).
9. CV is defined as the ratio of the standard deviation to the mean. The correlation coefficient was 0.65 ($P < 0.001$).
10. R. W. Kullberg, T. L. Lentz, M. W. Cohen, *Dev. Biol.* **60**, 101 (1977); Y. Kidokoro and E. Yeh, *Proc. Natl. Acad. Sci. U.S.A.* **79**, 6727 (1982); I. Chow and M.-m. Poo, *J. Neurosci.* **5**, 1076 (1985).
11. Z. Xie and M.-m. Poo, *Proc. Natl. Acad. Sci. U.S.A.* **83**, 7069 (1986); J. Evers, M. Laser, Y. Sun, Z-p. Xie, M.-m. Poo, *J. Neurosci.* **9**, 1523 (1989).
12. J. T. R. Isaac, R. A. Nicoll, R. C. Malenka, *Neuron* **15**, 427 (1995); D. Liao, N. A. Hessler, R. Malinow, *Nature* **375**, 400 (1995); G. M. Durand, Y. Kovalchuk, A. Konnerth, *ibid.* **381**, 71 (1996).
13. Data not shown.
14. Fluo-3 (pentapotassium salt; 200 μM in the pipette solution) was loaded into the myocyte with the whole-cell patch-recording pipette. After 10 min of loading, the loading pipette was detached and a perforated whole-cell patch recording was made and maintained under voltage clamp ($V_c = -70$ mV) during subsequent imaging of the cell. We monitored fluo-3 fluorescence with an oil-immersion objective (×40; numerical aperture, 1.3) coupled to a cooled charge-coupled device camera. We used a fluorescein filter set together with neutral density filters to adjust the level of excitation light. In each experiment, three 15-s episodes (60 frames grabbed at 4 Hz) of fluorescence images were acquired with imaging software. Two control episodes without burst stimulation were obtained 1 min before and 1 min after the test episode. In the test episode, we applied a burst stimulation 3 s after the start of the episode. In the image analysis for each episode, the fluorescence intensity of the entire myocyte was measured for each frame and normalized by the average intensity during the first 3 s. We averaged the change of normalized light intensity from two control episodes to obtain the photobleaching rate, which we subtracted from values obtained during the test episode.
15. F. A. Lai, H. P. Erickson, E. Rousseau, Q. Y. Liu, G. Meissner, *Nature* **331**, 315 (1988); S. J. Smith *et al.*, *J. Gen. Physiol.* **92**, 1 (1988); B. E. Ehrlich and J. Watras, *Nature* **336**, 583 (1988).
16. C. B. Klee, T. H. Crouch, M. H. Krinks, *Proc. Natl. Acad. Sci. U.S.A.* **76**, 6270 (1979); F. Shibasaki, E. R. Price, D. Milan, F. McKeon, *Nature* **382**, 370 (1996); C. B. Klee, H. Ren, X. Wang, *J. Biol. Chem.* **273**, 13367 (1998).
17. R. M. Mulkey, C. E. Herron, R. C. Malenka, *Science* **261**, 1051 (1993); R. M. Mulkey, S. Endo, S. Shenolikar, R. C. Malenka, *Nature* **369**, 486 (1994).
18. Calcineurin autoinhibitory peptide (CaN-AIP) and [Ala^{286}]calmodulin kinase II inhibitor(281–301) were obtained from Calbiochem (La Jolla, CA).
19. We induced persistent synaptic depression by photoactivated release of Ca^{2+} in nitr-5-loaded myocytes (*5*). This depression was prevented when the peptide inhibitor {[Ala^{286}]Ca^{2+}calmodulin kinase II inhibitor(281–301); Calbiochem} of CaMKII (200 μM) was loaded into the myocyte together with nitr-5 (J. Wan and M-m Poo, unpublished data).
20. R. C. Malenka *et al.*, *Nature* **340**, 554 (1989); R. Malinow, H. Schulman, R. W. Tsien, *Science* **245**, 862 (1989); A. J. Silva, C. F. Stevens, S. Tonegawa, Y. Wang, *ibid.* **257**, 201 (1992); J. Lisman, R. C. Malenka, R. A. Nicoll, R. Malinow, *ibid.* **276**, 2001 (1997).
21. L. T. Landmesser and M. J. O'Donovan, *J. Physiol. London* **347**, 189 (1984); M. J. O'Donovan, P. Wenner, N. Chub, J. Tabak, J. Rinzel, *Ann. N.Y. Acad. Sci.* **860**, 130 (1998).

22. Supported by a grant from the National Institutes of Health (NS22764). We thank C. F. Stevens and N. C. Spitzer for helpful suggestions and A. Schinder and B. Berninger for comments on the manuscript.

9 June 1999; accepted 4 August 1999